

Modification of the thioglycosyl–naphthalimides as potent and selective human O-GlcNAcase inhibitors

Shengqiang Shen, Lili Dong, Wei Chen, Xiangdi Zeng, Huizhe Lu, Qing Yang, and Jianjun Zhang

ACS Med. Chem. Lett., **Just Accepted Manuscript** • DOI: 10.1021/acsmchemlett.8b00406 • Publication Date (Web): 15 Nov 2018

Downloaded from <http://pubs.acs.org> on November 18, 2018

Just Accepted

“Just Accepted” manuscripts have been peer-reviewed and accepted for publication. They are posted online prior to technical editing, formatting for publication and author proofing. The American Chemical Society provides “Just Accepted” as a service to the research community to expedite the dissemination of scientific material as soon as possible after acceptance. “Just Accepted” manuscripts appear in full in PDF format accompanied by an HTML abstract. “Just Accepted” manuscripts have been fully peer reviewed, but should not be considered the official version of record. They are citable by the Digital Object Identifier (DOI®). “Just Accepted” is an optional service offered to authors. Therefore, the “Just Accepted” Web site may not include all articles that will be published in the journal. After a manuscript is technically edited and formatted, it will be removed from the “Just Accepted” Web site and published as an ASAP article. Note that technical editing may introduce minor changes to the manuscript text and/or graphics which could affect content, and all legal disclaimers and ethical guidelines that apply to the journal pertain. ACS cannot be held responsible for errors or consequences arising from the use of information contained in these “Just Accepted” manuscripts.



Modification of the thioglycosyl–naphthalimides as potent and selective human O-GlcNAcase inhibitors

Shengqiang Shen,[†] Lili Dong,[†] Wei Chen,[‡] Xiangdi, Zeng,[†] Huizhe Lu,[†] Qing Yang,^{*,‡,§} and Jianjun Zhang^{*,†}

[†]Department of Applied Chemistry, College of Science, China Agricultural University, Beijing, China

[‡]Institute of Plant Protection, Chinese Academy of Agricultural Sciences, Beijing 100193, China

[§]School of Life Science and Biotechnology, Dalian University of Technology, Dalian, China.

KEYWORDS: Thioglycosides, naphthalimids, human O-GlcNAcase, β -N-acetylhexosaminidase, inhibitor, docking, MD simulations

ABSTRACT: β -N-acetylhexosaminidases are widely distributed exo-glycosidases and have attracted significant attention due to their important roles in the field of pesticide and drug discovery. Remarkably, human O-GlcNAcase (hOGA) and human β -N-acetylhexosaminidase (HsHex) possess the same catalytic mechanism but play different physiological actions *in vivo*. In this article, we aim to improve the inhibitory potency and selectivity of previously reported thioglycosyl-naphthalimides against hOGA. The rational compound design led to the synthesis of **13r** bearing a 4-piperidynaphthalimide moiety as a highly potent hOGA inhibitor ($K_i = 0.6 \mu\text{M}$ against hOGA) with good selectivity ($K_i > 100 \mu\text{M}$ against HsHexB). Furthermore, to investigate the basis for the potency and selectivity of **13r** against hOGA, the possible inhibitory mechanisms of selected inhibitors (**15b**, **13b** and **13r**) against hOGA and HsHexB were studied using molecular docking and MD simulations. These 4-substituted naphthalimide thioglycosides may potentially serve as useful tools for the further study of the function of hOGA.

β -N-acetylhexosaminidases represent an important class of enzymes found in a number of organisms and are involved in diverse physiological functions including human autoimmune diseases¹⁻², fungi cell differentiation³, and insect morphogenesis⁴. Inhibitors of these enzymes are particularly useful in the regulation of corresponding bioprocesses, providing benefits in the development of eco-friendly pesticides or therapeutic drugs.⁵ Remarkably, two types of significant human β -N-acetylhexosaminidases, namely human O-GlcNAcase (hOGA, a family GH84 glycoside hydrolase) and human β -N-acetylhexosaminidase (HsHex, a family GH20 glycoside hydrolase) have been reported as potential pharmacological targets.⁶⁻⁷ These two enzymes follow the same substrate-assisted catalysis mechanism but play different pivotal roles *in vivo*.⁸

Human O-GlcNAcase (hOGA) is responsible for catalyzing the removal of O-GlcNAc from serine or threonine residues in nucleocytoplasmic proteins.⁸ The related O-GlcNAcylation is mediated by O-GlcNAc transferase (OGT) and O-GlcNAcase (OGA) under tightly regulated conditions.⁹ Dysregulation of O-GlcNAcylation cycling has been found to be closely linked to diseases such as Alzheimer's disease (AD)¹⁰⁻¹¹, cancer¹², and obesity¹³. It is worth noting that crystallographic investigations on hOGA in three recent reports¹⁴⁻¹⁶ laid a solid foundation for hOGA-related drug discovery. Human β -N-acetylhexosaminidase (HsHex) is found to be implicated in osteoarthritis and lysosomal storage disorders.¹

It has already been shown that small molecule inhibitors with good potency and selectivity towards one of these β -N-acetylhexosaminidases are of great importance to help in the treatment of correlated diseases.¹⁷ Inhibitors against β -N-acetylhexosaminidases can be classified as NAG-thiazoline¹⁸, PUGNAc¹⁹, Nagstatin²⁰, iminocyclitols²¹ and

naphthalimides²²⁻²⁶. Among these inhibitors, naphthalimide inhibitors were first found by high-throughput screening²², and one of the compounds **M-31850** (**1**) was determined to exhibit a promising inhibitory potency against HsHex (K_i value of $3.2 \mu\text{M}$)²². Subsequently, non-carbohydrate-based naphthalimide derivatives, e.g. compound **7a** (**2**) synthesized by Qian and Yang, exhibited a higher inhibitory activity (K_i value of $0.6 \mu\text{M}$) against HsHex compared to **M-31850**.²³ Furthermore, **Q1** (**3**) was found to possess an equally potent inhibitory activity against both human β -N-acetylhexosaminidase HsHex (K_i value of $2.2 \mu\text{M}$) and insect β -N-acetylhexosaminidases OfHex1 (K_i value of $4.3 \mu\text{M}$).²⁴ To improve the selective inhibition against OfHex1, **Q2** (**4**) bearing a 4-dimethylamino group on the naphthalimide unit was designed and exhibited K_i values of $0.3 \mu\text{M}$ against OfHex1 and more than $100 \mu\text{M}$ against HsHex.²⁴ The complex crystal structure of OfHex1-**Q1** (PDB: 3WMB) and OfHex1-**Q2** (PDB: 3WMC) revealed that the 4-dimethylaminonaphthalimide moiety of **Q2** rotates approximately 180° (relative to naphthalimide moiety of **Q1**) and is tightly bound to the +1 subunit of OfHex1 via π - π stacking with Trp490.²⁴ On the other hand, relative to **Q1** the added dimethylamino group led to an increase in the steric hindrance for **Q2** to bind the -1 subsite of HsHex.²⁴ These results suggest that the 4-substituent at naphthalimide moiety may be crucial for the activity and selectivity of β -N-acetylhexosaminidases in the naphthalimides. (Figure 1)

We recently identified thioglycosyl-naphthalimide derivatives as promising lead compounds for β -N-acetylhexosaminidase inhibitors²⁵⁻²⁶, in which inhibitor **15b** (**5**, $K_i = 3.8 \mu\text{M}$ against hOGA; $K_i = 30.4 \mu\text{M}$ against HsHexB) exhibited a significant inhibitory activity against hOGA and a certain degree of selectivity towards these two enzymes²⁵. In addition, structure-activity relationship studies revealed that a

linker containing five to seven atoms between thioglycosyl and naphthalimide moiety would be beneficial to the efficiency against hOGA.²⁵ Considering the profound effects hOGA has on disease treatment, we further attempted to modify thioglycosyl-naphthalimide compounds as potent and selective hOGA inhibitors. (Figure 1)

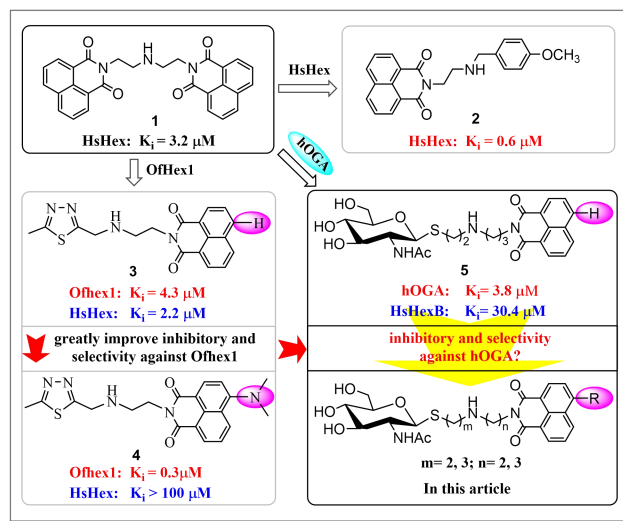


Figure 1. Design of 4-substituted naphthalimide thioglycosides for hOGA.

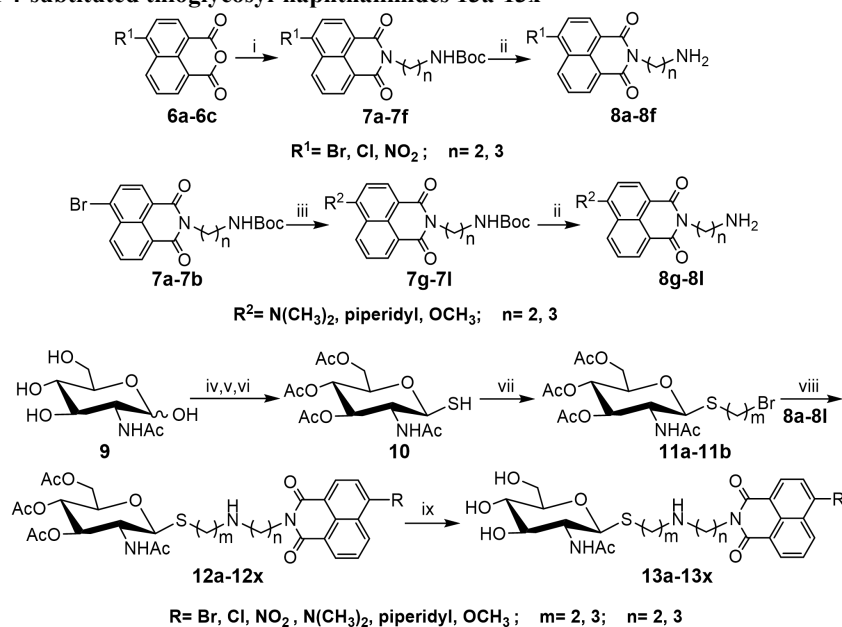
In this paper, we retained the frame structure of thioglycosyl-naphthalimides²⁵ and selected the length of the linker with five to seven atoms. Then, we focused on studying the influences of the 4-substituent group (on the naphthalimide moiety) on the inhibitory activity and selectivity against hOGA (Figure 1). Initially, our strategy involved the synthesis of a handful of 4-substituted naphthalimide thioglycosides and the measurement of the inhibition rates (or IC₅₀ values) towards hOGA and HsHex. This way, we could evaluate the potency of these thioglycosides rapidly and avoid unnecessary synthesis of a large number of compounds with uncertain activity. Thus, two thioglycosyl-naphthalimides, namely **13m** (bearing a 4-dimethylamino group) and **13c** (bearing a 4-bromo group), were synthesized and compared with the previously evaluated compounds²⁵ **15a** and **15d**. As shown in Table S1, in contrast to reference **15a**²⁵, even though **13m** showed a decreased potency against hOGA (IC₅₀ = 25.0 μM), it possessed good selectivity (IC₅₀ > 100 μM against HsHexB). In addition, **13c** was demonstrated to be approximately seven times more potent than **15d**²⁵, with an IC₅₀ value of 3.7 μM. These findings suggested that the 4-substituted group on the naphthalimide moiety exhibited a vital role in influencing the selectivity and potency of thioglycosyl-naphthalimides against hOGA. (Figure S1)

The list of observations described herein prompted us to further study the substituent residing in 4-position on the naphthalimide scaffold. Halogen substituents (Cl, Br), electron-donating groups (OCH₃, N(CH₃)₂), an electron-withdrawing group (NO₂) and a larger substituent (piperidyl) were introduced to the structure and the relationship between the inhibitory activity and the size or electronic properties of the substituents of these thioglycoside inhibitors were evaluated. In doing so, another 22 4-substituted naphthalimide thioglycosides with the linker containing five to seven atoms (m = 2, 3; n = 2, 3) were synthesized. As shown in Scheme 1,

thiol **10** could be prepared according to literature procedures in three steps.²⁷ Subsequently, **10** was reacted with α,ω-dibromoalkane to furnish the key intermediates **11a-11b** in acetone/water (2:1, v:v). Meanwhile, the naphthalimide derivatives **8a-8l** were obtained according to published methods (Scheme S1 and Scheme S2). Then, treatment of bromides **11a-11b** with naphthalimides **8a-8l** produced the acetyl-protected **12a-12x**. Finally, deacetylation of **12a-12x** via methanol-ammonia catalysis produced the target compounds **13a-13x** in 71-93% yield (Scheme S3).

Subsequently, these target compounds were evaluated for their inhibitory potency against hOGA and HsHexB by using 4-MU-GlcNAc as a substrate. The corresponding results are listed in Table 1 and Table 2. Analysis of **13a-13x** to assess the inhibitory activity against hOGA showed that the 4-substituted on the naphthalimide moiety exhibited a significant influence on the inhibitory activity. Specifically, the halogen substituents (Cl, Br) in 4-position on the naphthalimides (**13a-13h**) could slightly increase in inhibitory activity against hOGA compared to that of naphthalimides not bearing any 4-substituents (**15b**²⁵). However, compounds bearing a methoxy substituent (**13u-13x**) exhibited a minor activity decrease, and compounds bearing the nitro group (**13i-13l**) and dimethylamino group (**13m-13p**) demonstrated a significantly weakened inhibitory effect. It is suggested that the size of the 4-substituents may be the main factor to affect the inhibitory potency against hOGA rather than the electronic properties. In particular, the presence of smaller functional groups (Cl, Br) resulted in a more effective inhibitory potency than naphthalimides bearing OCH₃, NO₂, and N(CH₃)₂ substituents. In contrast, the presence of an electron-donating group (N(CH₃)₂) and electron-withdrawing group (NO₂) resulted in the same inhibitory activity. A special case was thioglycosyl-naphthalimides bearing piperidyl group (**13q-13t**) that featured a larger substituent than the dimethylamino group but exhibited the highest inhibitory potency against hOGA (**13r**, K_i = 0.6 μM). Presumably, the larger 4-piperidyl moiety may have led to a greater rotation of 4-piperidyl-naphthalimide to tightly bind to the relevant hydrophobic domain near the active pocket when interacting with hOGA. Furthermore, the relationship of inhibitory activity against hOGA and the flexible linker between the glycosyl and naphthalimide groups (values of m, n) exhibited a certain regularity. The inhibitors (**13b**, **13f**, **13r**, **13v** containing both thioethyl (m=2) and 3-aminopropyl-naphthalimide (n=3) exhibited a higher potency (e.g. **13r** > **13q**, **13s**, **13t**, Table 1).

The HsHexB inhibition of **13a-13x** (Table 1 and Table 2) revealed similar properties. The inhibitory potency of these compounds was also closely related to the size of 4-substituents residing on naphthalimide. The greater inhibitory activity of **13b** relative to **15b**²⁵ suggested that a slight increase in size of the 4-substituted on naphthalimide (from H to Br) could improve the binding affinity to HsHexB. However, upon increasing the size from halogen substituents (Cl, Br) to NO₂, N(CH₃)₂ and piperidyl substituents, a loss in activity was observed. These results show that a large substituent in this position may result in steric hindrance, ultimately decreasing the access of the inhibitors to enter the active pocket of the enzyme (HsHexB features a shallow substrate-binding pocket²⁴). It is worth mentioning that **13r** did not inhibit HsHexB but exhibited a hOGA inhibitory activity in the nanomolar range, which means in comparison with the classic inhibitor NGT, the thioglycosyl-naphthalimide **13r**

Scheme 1. Synthesis of 4-substituted thioglycosyl-naphthalimides **13a-13x**^a

^a Reagents and conditions: (i) tert-butyl (n-amino-alkyl) carbamate, EtOH; (ii) DCM, CF₃COOH; (iii) dimethylamine, 2-methoxyethanol for **7g**, **7h**; piperidine, 2-methoxyethanol for **7i**, **7j**; MeOH, K₂CO₃ for **7k**, **7l**; (iv) AcCl; (v) thiourea, acetone; (vi) Na₂S₂O₅, DCM, H₂O; (vii) **8a-8l**, K₂CO₃, acetone, H₂O; (viii) K₂CO₃, CH₃CN; (ix) NH₃, MeOH. m, n, R are defined in Table 1.

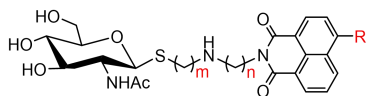
exhibited considerable inhibitory potency and with excellent selectivity for hOGA (Table 2).

Considering these interesting enzyme inhibition results of **15b**²⁵, **13b**, and **13r** (Table 2), we further studied how hOGA and HsHexB could recognize these compounds at the atomic level. Firstly, the dixon plots of **15b**²⁵, **13b**, and **13r** against hOGA and HsHexB were investigated (Figure S2). The data revealed that these active thioglycosyl-naphthalimides were competitive inhibitors and could specifically bind to the active pocket of the enzymes. Then, density functional theory (DFT) using the B3LYP/6-31G(d) basis set was performed to optimize the structures of **15b**²⁵, **13b**, and **13r** using the Gaussian 16 program (Figure S4). Subsequently, molecular docking with these optimized structures into the binding site of hOGA and HsHexB, respectively, were carried out using the complex crystal structure of hOGA-PUGNAc-type inhibitor (PDB ID: 5M7T)²¹ and HsHexB-NGT (PDB ID: 1NP0)²⁹. In an effort to shed further light on the appropriate interaction mode of **15b**²⁵, **13b**, and **13r** when bound to hOGA and HsHexB, we further implemented MD simulations of 30 ns, using structures generated from the docking. As shown in Figure 2a and Figure 2b, the root-mean-square deviations (RMSDs) of all structures between receptors and ligands were ultimately maintained around 2.0-3.0 Å. These data showed that equilibrated and converged stages were reached in these simulations. Besides, it could be observed that the hOGA and HsHexB receptors exhibited some larger fluctuations located at the loop areas of the proteins (Figure S5), which was in agreement with the high conformational flexibility of the glycoprotein.¹⁴

Superimposition of the conformations of **15b**²⁵ (green colored carbon atoms), **13b** (yellow colored carbon atoms), and **13r** (cyan colored carbon atoms) with hOGA at 30 ns of MD simulations are shown in Figure 2c. The glycosyl moiety from these three inhibitors was found to be tightly bound to the -1 subsite (active pocket) of hOGA and the naphthalimide

group extended out from the active pocket and interacted with residues of related hydrophobic domains. We then compared the binding modes of **15b**²⁵ (Figure S6a) and **13b** (Figure S6c) with hOGA. The results indicated that the hydrogen atom of NH in the 2-acetamido group of **13b** could establish key interactions with the catalytic residues G67 and W278 via hydrogen bonds and the 4-bromonaphthalimide moiety of **13b** rotated to the residue W679 to form a strong π - π stacking interaction as compared to **15b**²⁵. These interactions may have resulted in the 4-fold increase in hOGA inhibitory potency when compared with **15b**²⁵ and **13b**. For the binding mode of **13r** (Figure S6e), a significant conformational difference relative to **15b**²⁵ and **13b** could be observed. The naphthalimide moiety with a larger 4-piperidyl group of **13r** moved into the new hydrophobic domain, which was composed of F223, E677, P678, F681, W679, and the piperidyl group could then establish Van der Waals interactions with E677, P678 (Figure S6e). In addition, affected by the 4-piperidyl-naphthalimide moiety, the glycosyl moiety in **13r** entered more deeply into the hOGA pocket and the conformation of glycosyl rotated clockwise around 80°, relative to the glycosyl moiety in **15b**²⁵ (Figure 2c). Consequently, the key interactions could be observed due to the formation of hydrogen bonds between the catalytic residue N313 and the hydrogen atom in NH of the acetamido group in **13r** (Figure S6e). On the basis of these observations, **13r** possessed the most appropriate binding conformation for hOGA of these reported compounds, and thus exhibited the highest inhibitory potency.

In vitro assays revealed that **15b**²⁵, **13b**, and **13r** displayed a 8.0-, 2.0- and more than 167-fold higher selectivity for hOGA as compared to HsHexB (Table 2). Therefore, we sought to investigate this significant selectivity throughout the MD simulations. The conformations of the inhibitors **15b**²⁵, **13b**, and **13r** combined in the active pocket of HsHexB at 30 ns of MD simulations were extracted as shown in Figure 2d.

Table 1. Structures and hOGA as well as HsHexB inhibition rate of target compounds 13a-13x at a concentration of 20 μ M

Compd	substituent group			Inhibition rate (%)	
	R	m	n	hOGA	HsHexB
13a	Br	2	2	73.2 \pm 2.0	73.3 \pm 3.5
13b	Br	2	3	84.7 \pm 1.4	70.5 \pm 3.9
13c	Br	3	2	75.7 \pm 1.7	60.6 \pm 1.4
13d	Br	3	3	59.2 \pm 1.2	65.0 \pm 1.3
13e	Cl	2	2	66.1 \pm 1.5	73.8 \pm 2.7
13f	Cl	2	3	83.3 \pm 0.6	70.8 \pm 1.6
13g	Cl	3	2	83.6 \pm 2.3	75.2 \pm 3.2
13h	Cl	3	3	68.9 \pm 1.7	74.3 \pm 4.2
13i	NO ₂	2	2	25.1 \pm 2.1	13.8 \pm 1.8
13j	NO ₂	2	3	55.0 \pm 1.8	8.0 \pm 1.0
13k	NO ₂	3	2	25.6 \pm 2.6	0.0
13l	NO ₂	3	3	20.0 \pm 0.6	0.0
13m	N(CH ₃) ₂	2	2	32.6 \pm 1.8	0.0
13n	N(CH ₃) ₂	2	3	40.9 \pm 1.6	0.0
13o	N(CH ₃) ₂	3	2	26.6 \pm 3.0	0.0
13p	N(CH ₃) ₂	3	3	28.2 \pm 2.3	0.0
13q	piperidyl	2	2	36.7 \pm 1.8	0.0
13r	piperidyl	2	3	87.6 \pm 1.3	0.0
13s	piperidyl	3	2	67.5 \pm 2.5	0.0
13t	piperidyl	3	3	49.1 \pm 3.3	0.0
13u	OMe	2	2	56.4 \pm 1.8	22.5 \pm 1.1
13v	OMe	2	3	73.1 \pm 1.4	47.9 \pm 2.3
13w	OMe	3	2	34.3 \pm 3.1	39.0 \pm 2.8
13x	OMe	3	3	68.0 \pm 0.9	45.2 \pm 1.6
15b ^a	H	2	3	82.4 \pm 0.1	38.7 \pm 0.8

^aStructure and inhibition rate data of compound **15b** were taken from ref [25].

Compounds **15b**²⁵, **13b**, and **13r** exhibited significant differences in binding patterns. The binding mode between **15b**²⁵ and HsHexB (Figure S6b) showed that the naphthalimide group of **15b**²⁵ was bound to the active pocket of HsHexB via lesser interactions with W405, W489, E490 and the glycosyl moiety extended out from the pocket. In comparison with **15b**²⁵, as shown in Figure S6d, the glycosyl moiety from **13b** was found to be tightly bound to the active pocket via strong H-bonding interactions with residues R211, D290, E355, D354, E288. However, the naphthalimide group formed additional π - π stacking interactions with W489 outside of the pocket. These binding modes were coherent with the observed structure-activity relationship trend between **15b**²⁵ and **13b**, and, as a result, the increase in HsHexB inhibitory potency of **13b** led to the selectivity loss as compared to

Table 2. Inhibition constants and selectivity ratios of representative compounds for hOGA

Compd	K _i (μ M)		Selectivity ratio for hOGA
	hOGA	HsHexB	
13a	1.2 \pm 0.0	2.6 \pm 0.0	2.2
13b	0.9 \pm 0.0	1.8 \pm 0.1	2.0
13c	3.5 \pm 0.1	5.1 \pm 0.3	1.5
13d	2.2 \pm 0.1	4.4 \pm 0.1	2.0
13e	2.0 \pm 0.1	1.2 \pm 0.0	0.6
13f	0.8 \pm 0.1	1.6 \pm 0.1	2.0
13g	0.7 \pm 0.1	1.6 \pm 0.2	2.3
13h	2.1 \pm 0.1	1.8 \pm 0.2	0.9
13j	8.3 \pm 0.5	Nd	>12.0
13r	0.6 \pm 0.0	Nd	>167
13s	3.2 \pm 0.0	Nd	>31.2
13u	6.7 \pm 0.3	56.2 \pm 0.3	8.4
13v	1.6 \pm 0.1	22.1 \pm 0.0	13.8
13x	15.9 \pm 0.5	24.7 \pm 0.4	1.6
15b ^a	3.8 \pm 0.0	30.4 \pm 0.1	8.0
NGT	0.18 ^b	0.19 ^c	1.1

^aStructure and K_i values of **15b** were taken from ref [25]. ^bData was taken from ref [28]. ^cData was taken from ref [22]. Nd: not determined (less than 50% inhibition at 100 μ M).

hOGA. Furthermore, it is important to note that inhibitor **13r** showed notable differences in its position and conformation with HsHexB (Figure 2d). Both of the glycosyl and naphthalimide moieties of **13r** moved away from the active pocket (Figure S6f) resulting in contact loss with HsHexB. Accordingly, **13r** exhibited a significantly higher selectivity against hOGA as compared to HsHexB.

Table 3. Results of binding free energy calculated using the MM/GBSA method.

Compd	K _i (μ M)		ΔG_{GBTOT} (kcal/mol)	
	hOGA	HsHexB	hOGA	HsHexB
15b ^a	3.8	30.4	-27.9	-25.1
13b	0.9	1.8	-30.2	-27.4
13r	0.6	>100	-32.4	-16.7

^a Both structure and K_i values of compound **15b** were taken from ref [31].

To further explore the cause of the inhibitory potency and selectivity against hOGA, we performed binding free energy analyses of **15b**²⁵, **13b**, and **13r** using the MM/GBSA calculation methods and combined with MD simulations. The predicted energy values for MD trajectories from the last 4 ns can be found summarized in Table 3, exhibiting suitable consistency with the experimental hOGA and HsHexB inhibitory activities of **15b**²⁵, **13b**, and **13r**.

In summary, we reported the molecular design, synthesis, and inhibitory activities against hOGA and HsHexB of 4-substituted naphthalimide thioglycoside derivatives. Compared to our previously reported naphthalimide

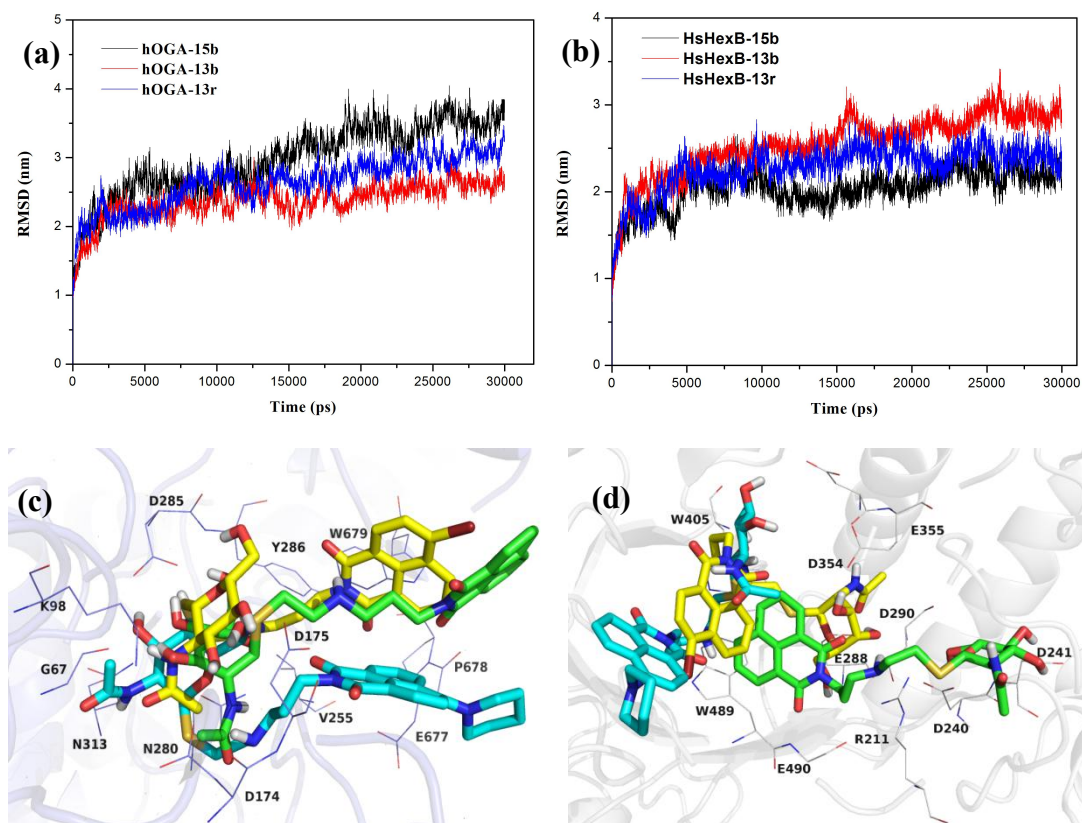


Figure 2. Predicted binding mechanism of thioglycosyl-naphthalimides **15b**²⁵, **13b**, and **13r** with hOGA (PDB ID:5M7T) and HsHexB (PDB ID:1NP0) revealed by molecular docking and MD simulations. RMSD changes of **15b**²⁵, **13b**, and **13r** in complex with hOGA (a) and HsHexB (b), respectively, during MD simulations. Binding modes of **15b**²⁵, **13b**, and **13r** with (c) hOGA and (d) HsHexB at 30 ns of MD simulations. **15b**²⁵ is shown in green, **13b** is shown in yellow, and **13r** is shown in cyan (colored by element).

thioglycosides, the 4-substituent group exerted a vital influence on both the potency and selectivity against hOGA. Particularly thioglycoside **13r** bearing a 4-piperidyl group exhibited the highest potency with a K_i value of 0.6 μM against hOGA and also exhibited excellent selectivity over HsHexB ($K_i > 100 \mu\text{M}$). Furthermore, molecular docking and MD simulations studies allowed us to rationalize the differences in potency and selectivity of the thioglycosyl-naphthalimides for hOGA. Taken in concert, the novel hOGA inhibitors reported here may find future applications as potential leads for the development of new therapeutic agents used in the treatment of hOGA-related diseases.

ASSOCIATED CONTENT

Supporting Information

The Supporting Information is available free of charge on the ACS Publications website.

Experimental procedures, enzymatic studies, molecular docking and MD simulations studies, and ¹H NMR and ¹³C NMR spectrum. (PDF)

AUTHOR INFORMATION

Corresponding Author

* E-mail: zhangjianjun@cau.edu.cn.

* E-mail: qingyang@dlut.edu.cn.

Author Contributions

The manuscript was written through contributions of all authors. All authors have given approval to the final version of the manuscript.

Notes

The authors declare no competing financial interest.

ACKNOWLEDGMENT

We acknowledge the financial support by the National Natural Science Foundation (21772230, 31425021) of China, and the National Key R&D Program (2018YFD0200100) of China.

ABBREVIATIONS

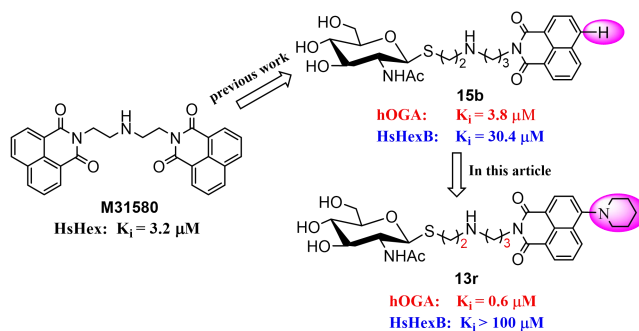
MD, molecular dynamics; DCM, dichloromethane; 4-MU-GlcNAc, 4-methylumbelliferyl N-acetyl- β -D-glucosaminide; NGT, NAG-thiazoline.

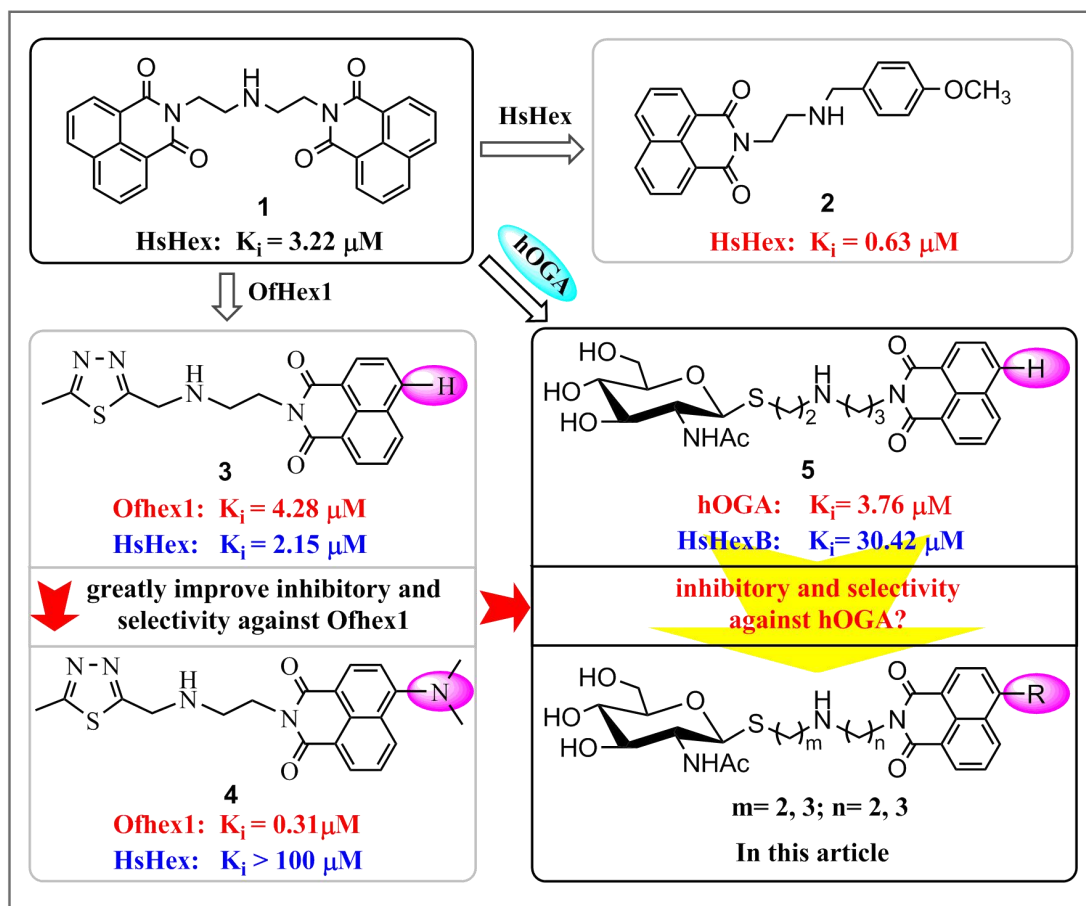
REFERENCES

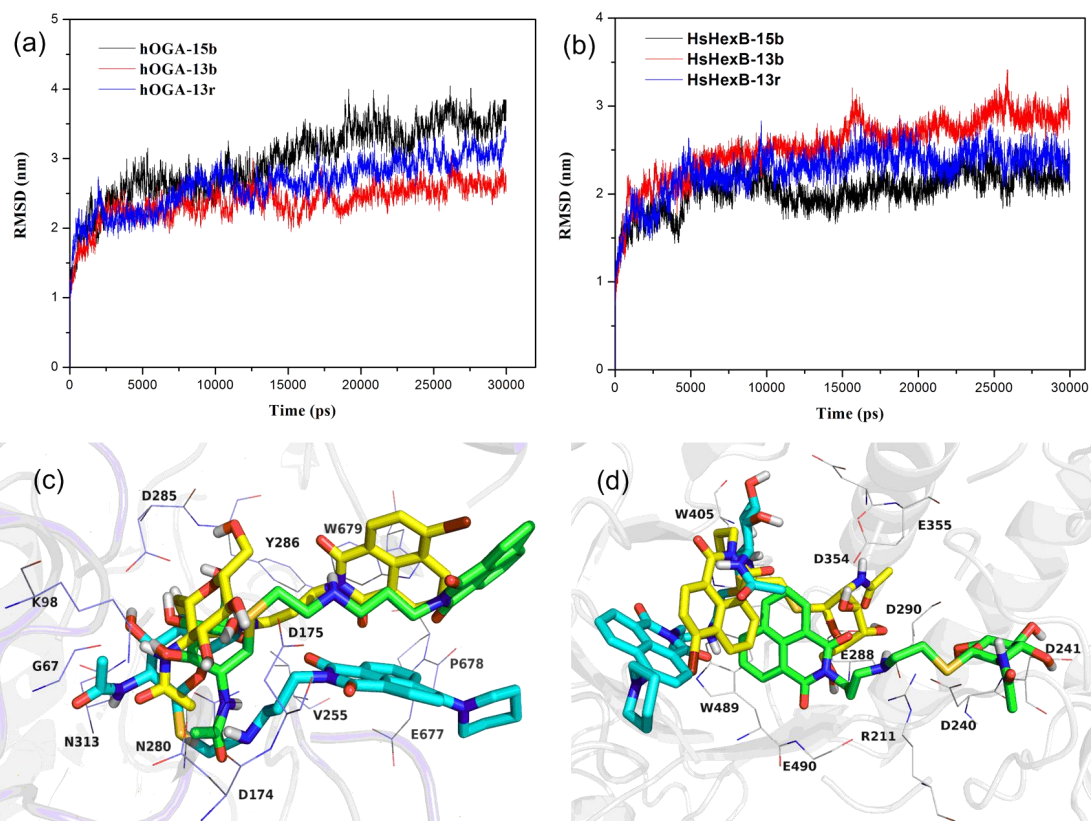
- Liu, J. J.; Shikhman, A. R.; Lotz, M. K.; Wong, C. H. Hexosaminidase inhibitors as new drug candidates for the therapy of osteoarthritis. *Chem. Biol.* **2001**, *8*, 701-711.
- Arnold, C. S.; Johnson, G. V. W.; Cole, R. N.; Dong, D. L. Y.; Lee, M.; Hart, G. W. The microtubule-associated protein tau is extensively modified with O-linked N-acetylglucosamine. *J. Biol. Chem.* **1996**, *271*, 28741-28744.
- Hartl, L.; Zach, S.; Seidl-Seiboth, V. Fungal chitinases: diversity, mechanistic properties and biotechnological potential. *Appl. Microbiol. Biot.* **2012**, *93*, 533-543.

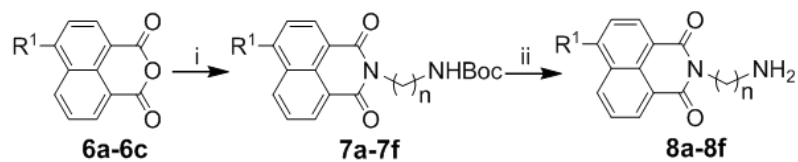
4. Liu, T.; Zhang, H.-T.; Liu, F.-Y.; Wu, Q.-Y.; Shen, X.; Yang, Q. Structural determinants of an insect β -N-Acetyl-D-hexosaminidase specialized as a chitinolytic enzyme. *J. Biol. Chem.* **2011**, *286*, 4049-4058.
5. Liu, T.; Chen, L.; Ma, Q.; Shen, X.; Yang, Q. Structural insights into chitinolytic enzymes and inhibition mechanisms of selective inhibitors. *Curr. Pharm. Design* **2014**, *20*, 754-770.
6. Zhu, Y.; Shan, X.; Safarpour, F.; Erro Go, N.; Li, N.; Shan, A.; Huang, M. C.; Deen, M.; Holicek, V.; Ashmus, R.; Madden, Z.; Gorski, S.; Silverman, M. A.; Vocadlo, D. J. Pharmacological inhibition of O-GlcNAcase enhances autophagy in brain through an mTOR-Independent pathway. *ACS Chem. Neurosci.* **2018**, *9*, 1366-1379.
7. Ho, C. W.; Popat, S. D.; Liu, T. W.; Tsai, K. C.; Ho, M. J.; Chen, W. H.; Yang, A. S.; Lin, C. H. Development of GlcNAc-inspired iminocyclitols as potent and selective N-acetyl-beta-hexosaminidase inhibitors. *Acs Chem. Biol.* **2010**, *5*, 489-497.
8. Liu, T.; Yan, J.; Yang, Q. Comparative biochemistry of GH3, GH20 and GH84 β -N-acetyl-D-hexosaminidases and recent progress in selective inhibitor discovery. *Curr. Drug Targets* **2012**, *13*, 512-525.
9. Yuzwa, S. A.; Macauley, M. S.; Heinonen, J. E.; Shan, X.; Dennis, R. J.; He, Y.; Whitworth, G. E.; Stubbs, K. A.; McEachern, E. J.; Davies, G. J.; Vocadlo, D. J. A potent mechanism-inspired O-GlcNAcase inhibitor that blocks phosphorylation of tau in vivo. *Nat. Chem. Biol.* **2008**, *4*, 483-490.
10. Yuzwa, S. A.; Shan, X.; Macauley, M. S.; Clark, T.; Skorobogatko, Y.; Vosseller, K.; Vocadlo, D. J. Increasing O-GlcNAc slows neurodegeneration and stabilizes tau against aggregation. *Nat. Chem. Biol.* **2012**, *8*, 393-399.
11. Yuzwa, S. A.; Vocadlo, D. J. O-GlcNAc and neurodegeneration: biochemical mechanisms and potential roles in Alzheimer's disease and beyond. *Chem. Soc. Rev.* **2014**, *43*, 6839-6858.
12. Ferrer, C. M.; Lynch, T. P.; Sodi, V. L.; Falcone, J. N.; Schwab, L. P.; Peacock, D. L.; Vocadlo, D. J.; Seagroves, T. N.; Reginato, M. J. O-GlcNAcylation regulates cancer metabolism and survival stress signaling via regulation of the HIF-1 pathway. *Mol. Cell* **2014**, *54*, 820-831.
13. McClain, D. A.; Lubas, W. A.; Cooksey, R. C.; Hazel, M.; Parker, G. J.; Love, D. C.; Hanover, J. A. Altered glycan-dependent signaling induces insulin resistance and hyperleptinemia. *Proc. Natl. Acad. Sci. USA.* **2002**, *99*, 10695-10699.
14. Elsen, N. L.; Patel, S. B.; Ford, R. E.; Hall, D. L.; Hess, F.; Kandula, H.; Kornienko, M.; Reid, J.; Selnick, H.; Shipman, J. M.; Sharma, S.; Lumb, K. J.; Soisson, S. M.; Klein, D. J. Insights into activity and inhibition from the crystal structure of human O-GlcNAcase. *Nat. Chem. Biol.* **2017**, *13*, 613-615.
15. Li, B.; Li, H.; Lu, L.; Jiang, J. Structures of human O-GlcNAcase and its complexes reveal a new substrate recognition mode. *Nat. Struct. Mol. Biol.* **2017**, *24*, 362-369.
16. Roth, C.; Chan, S.; Offen, W. A.; Hemsworth, G. R.; Willems, L. I.; King, D. T.; Varghese, V.; Britton, R.; Vocadlo, D. J.; Davies, G. J. Structural and functional insight into human O-GlcNAcase. *Nat. Chem. Biol.* **2017**, *13*, 610-612.
17. Glawar, A. F. G.; Martinez, R. F.; Ayers, B. J.; Hollas, M. A.; Ngo, N.; Nakagawa, S.; Kato, A.; Butters, T. D.; Fleet, G. W. J.; Jenkinson, S. F. Structural essentials for β -N-acetylhexosaminidase inhibition by amides of prolines, pipercolic and azetidone carboxylic acids. *Org. Biomol. Chem.* **2016**, *14*, 10371-10385.
18. Kong, H.; Chen, W.; Lu, H.; Yang, Q.; Dong, Y.; Wang, D.; Zhang, J. Synthesis of NAG-thiazoline-derived inhibitors for β -N-acetyl-D-hexosaminidases. *Carbohydr. Res.* **2015**, *413*, 135-144.
19. Hattie, M.; Cekic, N.; Debowski, A. W.; Vocadlo, D. J.; Stubbs, K. A. Modifying the phenyl group of PUGNAc: reactivity tuning to deliver selective inhibitors for N-acetyl-D-glucosaminidases. *Org. Biomol. Chem.* **2016**, *14*, 3193-3197.
20. Terinek, M.; Vasella, A. Synthesis of N-acetylglucosamine-derived nagstatin analogues and their evaluation as glycosidase inhibitors. *Helv. Chim. Acta.* **2005**, *88*, 10-22.
21. Ayers, B. J.; Glawar, A. F. G.; Martinez, R. F.; Ngo, N.; Liu, Z.; Fleet, G. W. J.; Butters, T. D.; Nash, R. J.; Yu, C. Y.; Wormald, M. R.; Nakagawa, S.; Adachi, I.; Kato, A.; Jenkinson, S. F. Nine of 16 stereoisomeric polyhydroxylated proline amides are potent β -N-acetylhexosaminidase inhibitors. *J. Org. Chem.* **2014**, *79*, 3398-3409.
22. Tropak, M. B.; Blanchard, J. E.; Withers, S. G.; Brown, E. D.; Mahuran, D. High-throughput screening for human lysosomal beta-N-Acetyl hexosaminidase inhibitors acting as pharmacological chaperones. *Chem. Biol.* **2007**, *14*, 153-64.
23. Guo, P.; Chen, Q.; Liu, T.; Xu, L.; Yang, Q.; Qian, X. Development of unsymmetrical dyads as potent noncarbohydrate-based inhibitors against human β -N-Acetyl-d-hexosaminidase. *ACS Med. Chem. Lett.* **2013**, *4*, 527-531.
24. Liu, T.; Guo, P.; Zhou, Y.; Wang, J.; Chen, L.; Yang, H.; Qian, X.; Yang, Q. A crystal structure-guided rational design switching non-carbohydrate inhibitors' specificity between two β -GlcNAcase homologs. *Sci. Rep.* **2014**, *4*, 6188-6183.
25. Shen, S.; Chen, W.; Dong, L.; Yang, Q.; Lu, H.; Zhang, J. Design and synthesis of naphthalimide group-bearing thioglycosides as novel β -N-acetylhexosaminidases inhibitors. *J. Enzyme Inhib. Med. Chem.* **2018**, *33*, 445-452.
26. Chen, W.; Shen, S.; Dong, L.; Zhang, J.; Yang, Q. Selective inhibition of β -N-acetylhexosaminidases by thioglycosyl-naphthalimide hybrid molecules. *Bioorg. Med. Chem.* **2018**, *26*, 394-400.
27. Paul, B.; Korytnyk, W. S., N-, and O-glycosyl derivatives of 2-acetamido-2-deoxy-D-glucose with hydrophobic aglycons as potential chemotherapeutic agents and N-acetyl- β -D-glucosaminidase inhibitors. *Carbohydr. Res.* **1984**, *126*, 27-43.
28. Krejzova, J.; Simon, P.; Kalachova, L.; Kulik, N.; Bojarova, P.; Marhol, P.; Pelantova, H.; Cvacka, J.; Etrich, R.; Slamova, K.; Kren, V. Inhibition of GlcNAc-processing glycosidases by C-6-azido-NAG-thiazoline and its derivatives. *Molecules* **2014**, *19*, 3471-3488.
29. Mark, B. L.; Mahuran, D. J.; Cherney, M. M.; Zhao, D.; Knapp, S.; James, M. N. G. Crystal structure of human β -Hexosaminidase B: Understanding the molecular basis of Sandhoff and Tay-Sachs disease. *J. Mol. Biol.* **2003**, *327*, 1093-1109.

β -N-acetylhexosaminidases are widely distributed exo-glycosidases and have attracted significant attention due to their important roles in the field of pesticide and drug discovery. Remarkably, human O-GlcNAcase (hOGA) and human β -N-acetylhexosaminidase (HsHex) possess the same catalytic mechanism but exhibit different physiological activities *in vivo*. In this article, we aim to improve the inhibitory potency and selectivity of previously reported thioglycosyl-naphthalimides against hOGA. Rational compound design led to the synthesis of **13r** bearing a 4-piperidyl-naphthalimide moiety as a highly potent hOGA inhibitor ($K_i = 0.6 \mu\text{M}$ against hOGA) with good selectivity ($K_i > 100 \mu\text{M}$ against HsHexB). Furthermore, to investigate the basis for the potency and selectivity of **13r** against hOGA, the possible inhibitory mechanisms of selected inhibitors (**15b**, **13b** and **13r**) against hOGA and HsHexB were studied using molecular docking and MD simulations. These 4-substituted naphthalimide thioglycosides may potentially serve as useful tools for the further study of the function of hOGA.

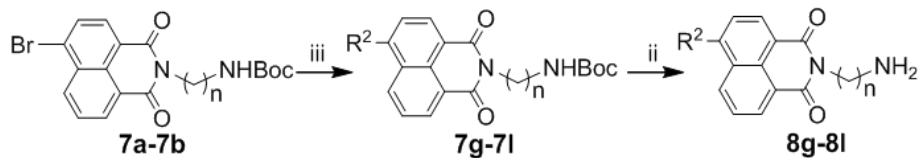




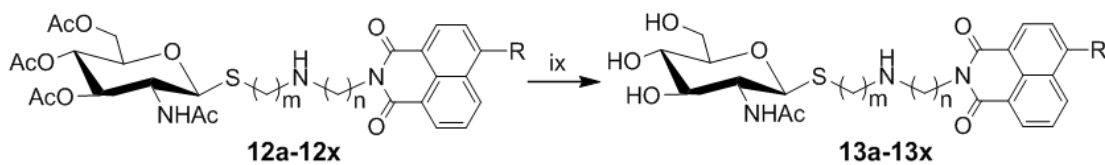
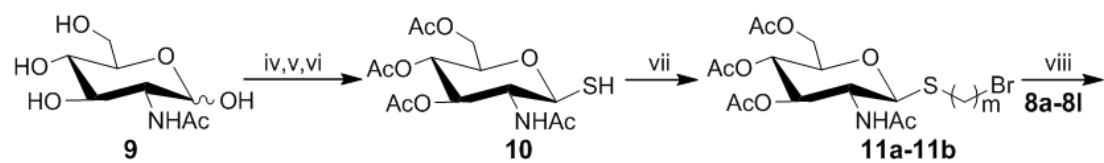




$R^1 = \text{Br, Cl, NO}_2$; $n = 2, 3$



$R^2 = \text{N(CH}_3)_2, \text{piperidyl, OCH}_3$; $n = 2, 3$



$R = \text{Br, Cl, NO}_2, \text{N(CH}_3)_2, \text{piperidyl, OCH}_3$; $m = 2, 3$; $n = 2, 3$